Catalysis Letters
https://doi.org/10.1007/s10562-020-03131-0

Spinel Structured Copper Ferrite Nano Catalyst with Magnetic Recyclability for Oxidative Decarboxylation of Phenyl Acetic Acids

Taskia Rahman[1] · **Geetika Borah**[1] · **Pradip K. Gogoi**[1]

Received: 11 November 2019 / Accepted: 31 January 2020
© Springer Science+Business Media, LLC, part of Springer Nature 2020

Abstract

A simple, efficient and environmentally benign method has been discussed for the synthesis of aldehydes and ketones by the oxidative decarboxylation of phenylacetic acid under ligand free condition using simple, efficient, preparatively easy, magnetically recoverable and low cost spinel $CuFe_2O_4$ nanoparticles. The catalyst was characterised using powder-XRD, FTIR, FE-SEM, EDX, VSM and HRTEM. The recyclability was examined and the results showed that the catalyst remained almost equally active up to five consecutive cycles.

Graphic Abstract

Spinel Structured Copper Ferrite is a very efficient nano catalyst for Oxidative decarboxylation of Phenyl acetic acids and can be reused up to five cycles without significant loss in catalytic activity.

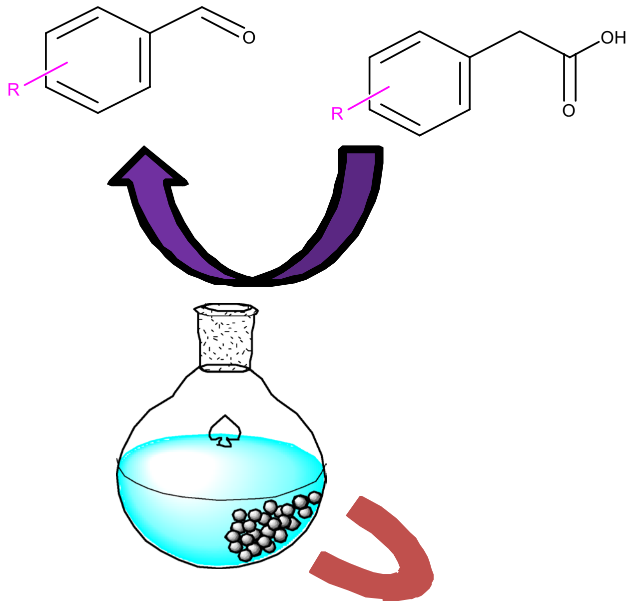

Keywords Heterogeneous catalysis · Oxidative decarboxylation · Phenyl acetic acid · Magnetic nanoparticles

1 Introduction

In contemporary time, the transition metal catalyzed C–C bond cleavage has been emerged as one of the most significant reaction in organic chemistry. The selective cleavage of the C–C bond is a remarkable challenge for synthetic

---

Electronic supplementary material The online version of this article (https://doi.org/10.1007/s10562-020-03131-0) contains supplementary material, which is available to authorized users.

Extended author information available on the last page of the article

Published online: 12 February 2020

chemists and biologists as well due to the inert nature of C–C σ-bonds. In a multistep reaction sequence decarboxylation of organic acids is one of the most important reactions in organic synthesis. Among all types of the reactions, functional group introduction at sp^3-hybridized carbon by decarboxylation is rare and remains a major challenge compared to sp^2-hybridized carbon which is mostly explored in the literature [1–5]. Researchers are attracted towards transition-metal-catalyzed decarboxylation reactions due to readily accessible starting materials, operational simplicity, and clean byproduct. In the past few years Liu and his co-workers developed several Pd-catalyzed decarboxylations using different types of aliphatic carboxylate salts [6–8], however the direct transition-metal-catalyzed decarboxylation of sp^3-hybridized carboxylic acids with the formation of a new C=O bond in the adjacent carbon using molecular oxygen as the oxidant is rare [9, 10]. But, Pd-catalyzed methods suffer from various disadvantages like Pd is expensive, air or moisture sensitive, and phosphines are mostly required for the success of the reactions. Thus, much attention has been paid towards designing more promising, greener, efficient, environmentally benign and economically feasible protocol for the aforementioned transformation is still in search. In the present decade remarkable progress has been made with copper catalyzed reactions and strikingly very few reports have been published in the field of oxidative decarboxylation reactions namely, Song and co-workers developed the ability of cupric salts for oxidative decarboxylation at sp^3-hybridized carbon to afford aldehydes, ketones [1] and amides [11] at high temperatures in presence of oxygen as oxidant. Recently, Pahari et al. [12] have demonstrated aerobic oxidative decarboxylation of phenylacetic acids by cellulose-supported Ag-Ag_2S nanoparticles. Thus, development of a recyclable and recoverable metal catalytic system capable of carrying out decarboxylation at sp^3-carbon centres under ligand and base free condition seems important. The development of economically feasible, eco-friendly and easily retrievable catalytic system has become a topic of apex priority in industrial and academic domains. In recent years researchers are interested towards metal oxide nanoparticles and mixed oxide spinel nanoparticles have received increased attention because of their wide range of applications in ultra-high magnetic data storage, magnetic resonance imaging, sorbents, drug delivery, catalysts, bio sensing, nano-electronic materials, electronics industry (electrodes and superconductors), etc. [13–17]. The mixed metal oxide spinels showed comparatively better catalytic activity in different transformations, viz. CO oxidation [18, 19], hydrocarbon combustion [20] and redox reactions of organic compounds [21]. Strikingly, magnetic spinel nanoparticles have gained wide attention in the present decade because of its significant advantages such as remarkable catalytic activity, easy preparation, operational simplicity, environmentally benign, and recoverability with an external magnetic field [22–24]. To prevent the loss of catalyst and enhances reusability, magnetic separation is an attractive choice to filtration or centrifugation and also promising material for various fields such as biomedicine, biotechnology and materials science. These distinct advantages of magnetic metal oxide nanoparticles in addition to continuation of our research interest in transition-metal-catalyzed organic reactions [25, 26] triggered us to develop magnetically recoverable copper ferrite spinel nanoparticles for the oxidative decarboxylation reaction of phenylacetic acid derivatives to aldehydes and ketone.

2 Experimental

2.1 Preparation of Copper Ferrite Nanoparticles

2.5 mmol of $Cu(NO_3)_2·3H_2O$ and 5.0 mmol of $Fe(NO_3)_3·9H_2O$ was dissolved in 10 mL of distilled water at 90 °C, followed by addition of 4 M NaOH solution drop wise to the mixture under vigorous magnetic stirring for 2 h. The resulting solution was centrifuged and washed several times with distilled water and acetone, followed by drying at 110 °C in an oven [22].

3 Results and Discussion

The position and relative intensities of all peaks confirm well with standard XRD (Fig. 1) pattern of $CuFe_2O_4$. The sharp diffraction peaks indicated crystalline nature of the $CuFe_2O_4$ spinel calcined at 500 °C. The diffraction

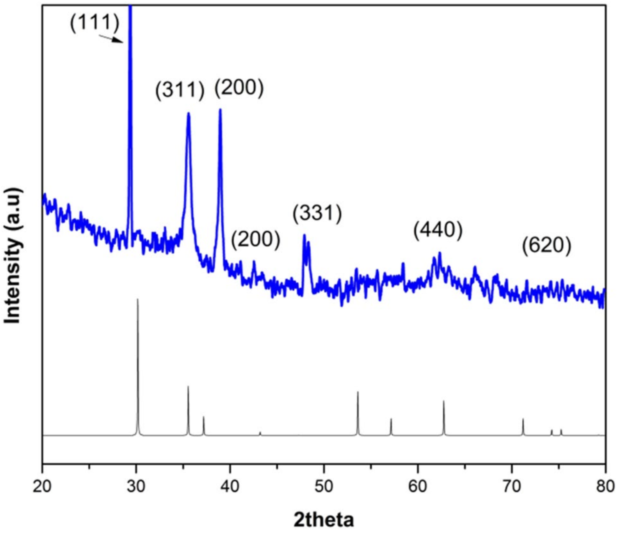

Fig. 1 XRD pattern of $CuFe_2O_4$

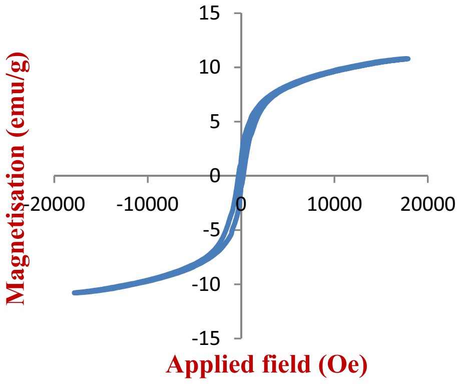

Fig. 2 Magnetic hysteresis loop of $CuFe_2O_4$

peaks of $CuFe_2O_4$ with 2θ values at 30.1°, 35.6°, 38.7°, 42.8°, 47.3°, 57.1°, 62.95°, 71.2° corresponds to the crystal planes (111), (311), (200), (200), (331), (511), (440), (620) planes, respectively and could be indexed to face centred cubic structure (JCPDS card number 34-0425). The crystallite size, calculated from XRD data based on the plane (111) at the 2θ value of 30.1° and using the Scherrer equation was found to be in 16 nm. The room temperature magnetic hysteresis curve (Magnetization and Field) of the sample shown in Fig. 2 was studied by a vibrating sample magnetometer. It exhibited a characteristic pattern of ferromagnetic component. As the driving magnetic field was dropped to zero the $CuFe_2O_4$ nano composite has still 1.2684 emu/g remanence value with coercivity value 260.56 Oe. The saturation magnetization was found to be 10.795 emu/g. This behaviour of the synthesized material unambiguously supports the presence of ferromagnetic component.

The FTIR spectrum of fresh catalyst (Fig. 3) shows a broad, medium intensity well-defined band at 580 cm^{-1} which suggests intrinsic stretching vibrations of the Fe–O bonds at the tetrahedral site and the weak peak at 451 cm^{-1} attributes to the Cu–O stretching vibration. The recycled catalyst exhibited quite similar bands in this region. Notably, observation of two absorption bands below 600 cm^{-1} is a universal feature of cubic spinel structure of ferrite materials. The bands at 1602 $cm^{-1}$and 3431 cm^{-1}(broad) could be attributed to the $\gamma_{\text{O–H}}$ and $\upsilon_{\text{O–H}}$ of water molecules and O–H groups, respectively [27, 28].

The TEM image (Fig. 4a) showed non homogeneous particle shape. The selected area electron diffraction (SAED) pattern exhibited sharp diffraction that indicated crystalline nature of the structure. The particle size distribution calculated from TEM image (Fig. 4b) showed narrow sized dispersion in the range of 2–18 nm. From TEM histogram, the average particle size of the nanoparticles was found to be 11 nm. The EDX analysis of spinel $CuFe_2O_4$ nanoparticles (Fig. 5) confirmed the presence of oxygen, iron and copper element with iron-copper ratio as approximately 2:1.

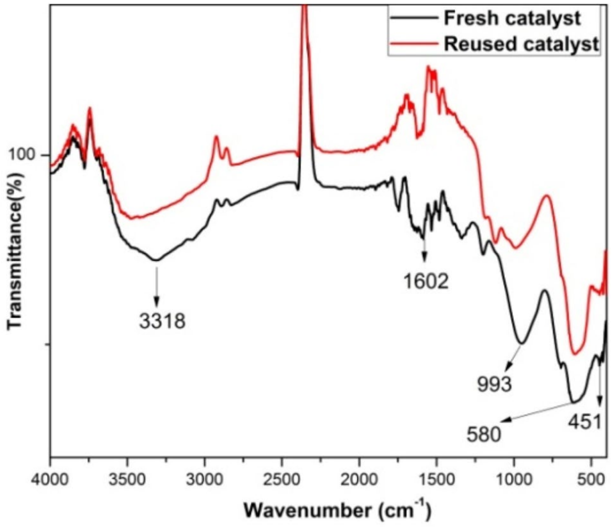

Fig. 3 FTIR spectra of fresh and reused $CuFe_2O_4$

To check catalytic activity of spinel $CuFe_2O_4$ we began our investigations taking phenylacetic acid as a model substrate (Table 1). It was observed that the reaction did not show detectable product formation even after prolonged time in H_2O both at room temperature (Table 1, entry 1) and elevated temperature (Table 1, entry 2). While the reaction was conducted in DMSO with 15 mol% catalyst at 120 °C for 12 h, the desired product was formed in 76% yield (Table 1, entry 4). On the other hand, in DMF the conversion was found to be 68% (Table 1, entry 7). Moreover, a blank reaction without catalyst showed non formation of product (Table 1, entry 9). Following the optimized reaction conditions, a number of different phenylacetic acid derivatives were studied. Phenylacetic acids bearing electron-donating groups on the aromatic rings gave the desired products in good to excellent yields (Table 2, entries-1, 7 and 11). Phenylacetic acids possessing electron-withdrawing groups (Table 2, entries-2–6 and 8–10) on the aromatic ring also reacted smoothly, and produced good to excellent yields of the desired aldehydes. The position of the substituents on the aromatic rings affected the product yield. Ortho-substitution usually giving lower yields of the aldehydes compared to meta- and para-substitution, which might be due to steric hindrance. Moreover, we have performed the reaction with benzoic acid and 4-amino benzoic acid but there is no product formation.

3.1 Catalyst reusability

The reusability of heterogeneous catalysts becomes a significant factor owing to strict economic and ecological

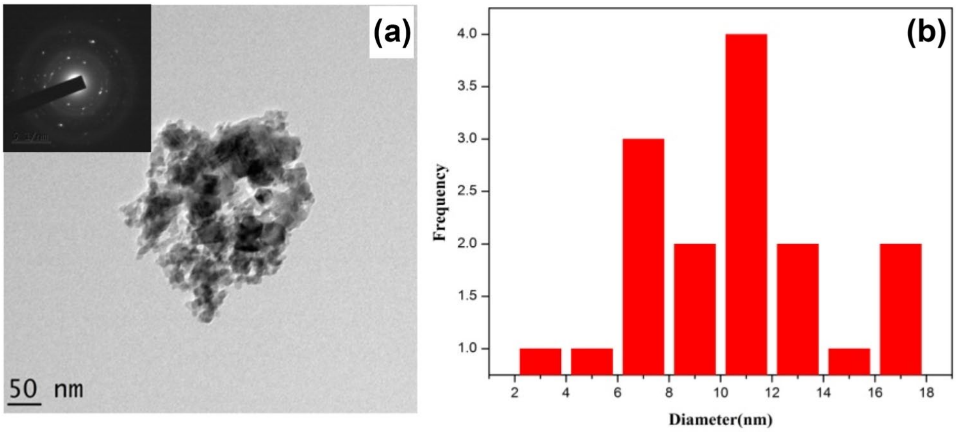

Fig. 4 **a** TEM image of fresh $CuFe_2O_4$ with SAED pattern (inset) **b** Particle size distribution histogram of $CuFe_2O_4$

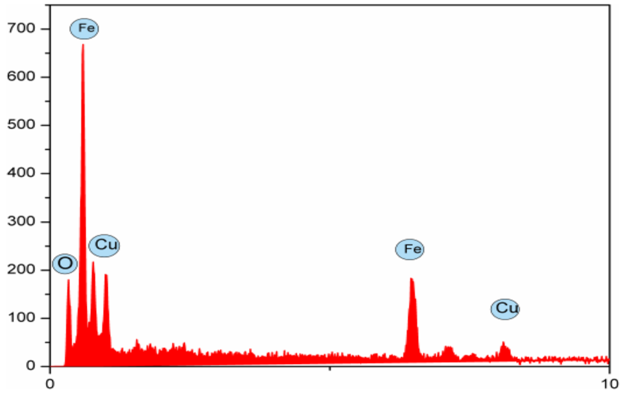

Fig. 5 SEM-EDX of $CuFe_2O_4$

demands for sustainability. Therefore, we have studied the possibility of recyclability of the catalyst. For this purpose the reaction of 4-(trifluoromethyl) phenyl acetic acid under optimized reaction conditions was selected (Fig S3, ESI). After completion of the reaction the catalyst was isolated from the reaction mixture by an external magnet, washed with diethyl ether and allowed to dry. After drying it was reused directly for the next run. The results indicated that the catalyst remained almost equally active up to five consecutive cycles.

3.2 Proposed reaction mechanism of oxidative decarboxylation

From the Scheme 1, it may be proposed that the phenylacetic acid was decarboxylated to give an active copper species with concomitant oxidation into corresponding aldehyde via the peroxy cuprate [1, 29].

Table 1 Screening of reaction conditions

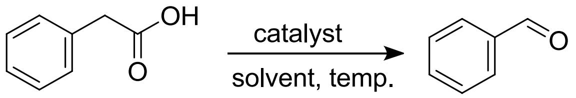

Entry	Solvent	Catalyst (mol%)	Oxidant	Temp (°C)	Yield (%)[a]
1	H_2O	10	H_2O_2	r.t	–
2	H_2O	20	H_2O_2	100	–
3	H_2O	15	H_2O_2	100	–
4	DMSO	15	H_2O_2	120	76
5	CH_3CN	20	H_2O_2	82	–
6	H_2O: CH_3CN	15	H_2O_2	100	–
7	DMF	15	H_2O_2	120	68
8	**DMSO**	**15**	**Air**	**120**	**76**
9	DMSO	–	Air	120	–
10	DMSO	15	Air	r.t	–
11	DMSO	15	Air	70	41
12	DMSO	15	Air	140	76
13	DMSO	12	Air	120	63

Phenyl acetic acid (1 mmol), Solvent (2–5 mL) catalyst (10–20 mol%), time (12 h)

[a] Isolated yield, Bold indicates optimised condition

4 Conclusion

In summary, magnetically separable spinel $CuFe_2O_4$ nanocatalyst has been prepared by co-precipitation method and extensively characterized. The particle size distribution calculated from TEM image showed narrow sized dispersion with an average particle size of 11 nm. The prepared catalyst was found to be very effective for oxidative decarboxylation of phenylacetic acids to corresponding aldehydes and ketones. The easy magnetic separation of the

Table 2 Substrate scope for oxidative decarboxylation reaction catalysed by spinel $CuFe_2O_4$

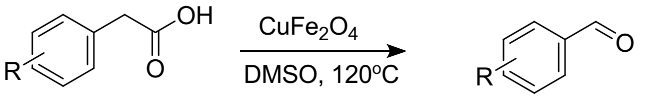

Entry	Substrate	Product	Time (h)	Yield (%) [a]
1	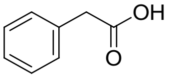	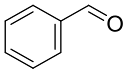	12	76
2	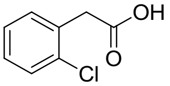	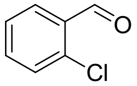	12	72
3	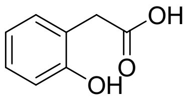	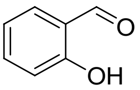	14	68
4	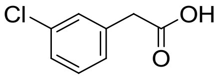	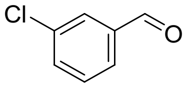	10	81
5	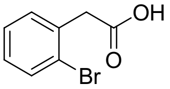	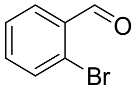	12	72
6	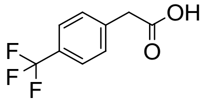	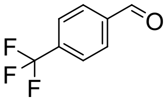	10	89
7	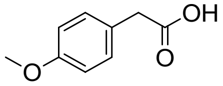	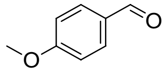	10	82
8	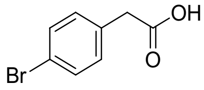	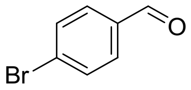	10	81
9	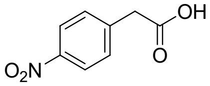	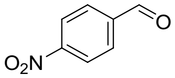	12	60
10	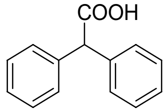	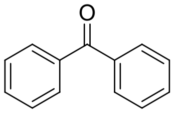	10	91
11	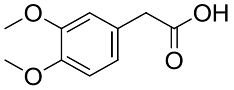	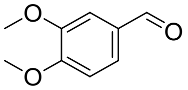	12	73

Reaction Conditions: Aryl acetic acid (1 mmol), catalyst (15 mol%), DMSO (2 mL), Temp (120°C)

[a] Isolated yield

catalyst from the reaction mixture eliminates the process of filtration and could be reused up to fifth consecutive cycle without remarkable loss in catalytic activity which is an additional green attribute of this reaction.

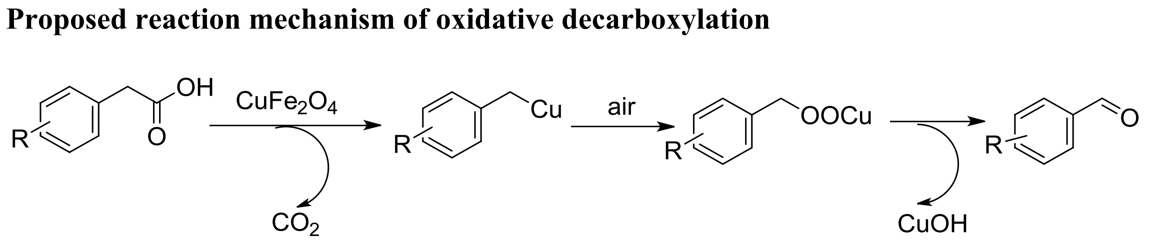

Scheme 1 Proposed reaction mechanism of oxidative decarboxylation

Acknowledgements The authors acknowledge the analytical services provided by STIC Kochi, SAIF NEHU Shillong, CIF IIT Guwahati, CSIC Dibrugarh University. The authors are also grateful to UGC, New Delhi, India for the financial support under the scheme SAP-DRS-I (2016-2021) and the Department of Science and Technology for financial assistance under the DST-FIST program.

References

1. Feng Q, Song Q (2014) J Org Chem 79:1867
2. Jun CH (2004) Chem Soc Rev 33:610
3. Dzik WI, Lange PP, Goossen L (2012) J Chem Sci 3:2671
4. Rodriguez N, Goossen L (2011) J. Chem. Soc. Rev. 40:5030
5. Mete TB, Khopade TM, Bhat RG (2017) Tetrahedron Lett 58:2822
6. Shang R, Yang ZW, Wang Y, Zhang SL, Liu L (2010) J Am Chem Soc 132:14391
7. Shang R, Huang Z, Chu L, Fu Y, Liu L (2011) Org Lett 13:4240
8. Shang R, Ji DS, Chu L, Fu Y, Liu L (2011) Angew Chem Int Ed 50:4470
9. Song Q, Feng Q, Zhou M (2013) Org Lett 15:5990
10. Feng Q, Song Q (2014) Adv Synth Catal 356:1697
11. Song Q, Feng Q, Yang K (2014) Org Lett 16:624
12. Hussain FL, Suri M, Namdeo A, Borah G, Dutta D, Goswami T, Pahari P (2019) Catal Commun 124:76
13. Kumar V, Mariappan CR, Azmi R, Moock D, Indris S, Bruns M, Ehrenberg H, Prakash GV (2017) ACS Omega 2:6003
14. Pendashteh A, Rahmanifar MS, Kaner RB, Mousavi MF (2014) Chem Commun 50:1972
15. Wu H, Lou Z, Yang H, Shen G (2015) Nanoscale 7:1921
16. Goyal A, Bansal S, Kumar V, Singh J, Singhal S (2015) Appl Surf Sci 324:877
17. Nassar MY, Khatab M (2016) RSC Adv. 6:79688
18. Ghose J, Murthy KSRC (1996) J Catal 162:359
19. Salker AV, Gurav SM (2000) J Mater Sci 35:4713
20. Hosseini SA, Niaei A, Salari D, Nabavi SR (2012) Ceram Int 38:1655
21. Zhai X, Yang W, Li M, Lv G, Liu J, Zhang X (2013) Carbon 65:277
22. Bazgir A, Hosseini G, Ghahremanzadeh R (2013) ACS Comb. Sci. 15:530
23. Zhang R, Miao C, Shen Z, Wang S, Xia C, Sun W (2012) ChemCatChem 4:824
24. Huynh MM, Do DP, Tran TN, Nguyen HKH, Tran HQ, Luu TX (2018) Catal Lett 148:924
25. Rahman T, Borah G, Gogoi PK (2019) J Chem Sci 131:4.
26. Rahman T, Borah G, Gogoi PK (2018) J Indian Chem Soc 95:795
27. Chavan P, Naik LR (2018) Sens. Actuators 272:28
28. Vergis BR, Krishna RH, Kottam N, Nagabhushana BM, Sharath R, Darukaprasad B (2018) J. Nanostruct. Chem. 8:1
29. Baruah D, Konwar D (2015) Catal Commun 69:68

Publisher's Note Springer Nature remains neutral with regard to jurisdictional claims in published maps and institutional affiliations.

Affiliations

Taskia Rahman[1] · Geetika Borah[1] · Pradip K. Gogoi[1]

✉ Geetika Borah
geetikachem@yahoo.co.in

✉ Pradip K. Gogoi
dr.pradip54@gmail.com

Taskia Rahman
rahmantaskia@gmail.com

[1] Department of Chemistry, Dibrugarh University, Dibrugarh, Assam, India